ELSEVIER

Applied Energy 73 (2002) 103–138

APPLIED ENERGY

www.elsevier.com/locate/apenergy

Raising the effectiveness of electricity generation (per unit of fossil-fuel combusted) by less conventional means

D. Dunstan*, D. Probert

School of Engineering, Cranfield University, Bedfordshire, MK43 0AL, UK

Accepted 20 August 2002

Abstract

Proposed, conceptual designs and applications for a cascaded system for electricity generation, employing "waste" heat from a primary stage as the stimulation for a subsequent stage, are outlined. The use of solar energy, wind and/or hydropower to supplement the energy inputs to the second and third stages is also considered. Present and future economic viabilities of the proposed hybrid electricity-generation systems are assessed qualitatively.

1. The challenge

As the unit costs of fossil fuels are set to rise significantly in the near future, the concept of "insolation assisting waste-heat" derived electric-power generation deserves consideration. Reflected and focussed insolation may be used to energise the working fluid in a stationary turbine, whereas the "waste" heat could be derived from a gas-turbine or diesel engine. This latter process may be desirable to reduce thermal pollution or to achieve a lower fire-hazard environment.

The "waste" heat emerging from a combined heat-and-power (CHP) unit is not usually converted into electrical power but employed as thermal energy because of the relatively-low conversion efficiencies achieved. Nevertheless, for some applications, e.g. in the tropics, "waste" heat often contributes to an already hot artificial environment, so it may be desirable to convert at least some of it into electricity. This will reduce calefaction (i.e. thermal pollution of the environment) as well as any 'Climate-Change' Levy liability that should be charged. Also, the thermal signature

* Corresponding author.

0306-2619/02/$ - see front matter
PII: S0306-2619(02)00076-4

Nomenclature and abbreviations

A	Area of magnet's pole surface (m^2)
AMP	Amperes
AM1	Maximum insolation at sea level (kWm^{-2})
B	Strength of the magnet ($Vs\ m^{-2}$)
C	Concentration power of CPC (see Fig. 3a)
C_P	Specific heat capacity ($J\ kg^{-1}\ K^{-1}$)
CCGT	Combined-cycle gas-turbine
CHP	Combined heat-and-power
CPC	Compound parabolic concentrator
CPP	Combined power plant
DIPPER	Double-irradiated photovoltaic and photon energy-relay
FP	Flat (solar-panel) plate
GWh	Giga Watt-hours
IHCPV	Integrated high-concentration photovoltaic-cell
kW_e	Kilowatt of electrical power
LPHW	Low-pressure hot-water
$\dot{m}$	Mass flow ($kg\ s^{-1}$)
MHD	Magnetohydrodynamic cycle
MW_e	Megawatt of electrical power
n	Refractive index of matter
N	Number of magnets
NIR	Near infrared
OCGT	Open-cycle gas-turbine
P	Pressure ($N\ m^{-2}$)
PV	Photovoltaic
r	Turbine blades' radius (m)
R	Specific gas constant ($J*kg^{-}\ k^{-1}$
RST	Reflective solar tower
T	Temperature (K)
TIR	Total internal reflection (in an insolation concentrator)
$\dot{V}$	Volumetric flow
W	Watts
δ	Volumetric coefficient ($= \dot{V}^2/r^2\dot{\phi}$)
η	Efficiency
$\dot{\theta}$	Frequency of rotating magnet (Hz)
$\dot{\phi}$	Rotational velocity of each turbine blade (radius s^{-1})

Glossary

Dichroic mirror	A mirror that reflects radiation of one wavelength but transmits radiation of other wavelengths.
KohinOr light extractor	A quartz-crystal optics-device used for concentrating received insolation.
Responsivity	A parameter indicating the electrical-power output of a solar photovoltaic cell per unit insolation input.

of a military unmanned spy aircraft [1] would then be much less noticeable (if a combined power and waste-heat derived power (CPP) unit were to be employed to provide the motive force) and hence its probability of detection by an enemy would be reduced.

However, in all cases, the prime aim should be to maximise the generation efficiency of the first stage of electricity generation (see Fig. 1), and then to maximise the efficiency of the subsequent stage using any suitable heat outputs from the first stage and other energy supplies. The same precedence priority should apply with respect to the second and third stages.

The present conceptual exercise is for qualitative purposes only. In practice, the presented electricity costs (in p/kWh) would be influenced by factors additional to those considered here, but nevertheless the present evaluated costs are useful for comparative purposes.

2. The prime mover

Several types of primary electricity-generators are in common use today, e.g. as combined-cycle gas-turbines (CCGTs) and open-cycle gas-turbines (OCGTs)—see Table 1 [2], as well as solar-energy converters [4].

For this conceptual study, an attempt has been made to increase the total electrical-power output (per unit of fuel expended) of a 3-stage generator-set by the use of a supplementary back-up system [5–8]. For this generalised 'paper' exercise, the generator-set should be capable of satisfying a wide range of electricity demands at all times by using a part of, or the entire, system at any location in the world. In practice, each cascaded system would be designed for a particular set of conditions, e.g. ambient environment and unit price of fuel used.

3. Small-scale insolation-harnessing by solar concentrators

Energy from the Sun is almost sustainable as far as we are concerned. The mean maximum solar flux (AM1) at sea level on Earth is $\sim$1 kW m^{-2}. Practical testing

has shown that a CCGT's working-fluid temperature of 1200 °C has been achieved with a concentrated insolation-flux rate of 10 MW m^{-2} [4].

Solar concentrators consist of a series of mirrors that focus the insolation into a single aperture. Modern apertures, made mostly of quartz, can achieve a 99% transmission efficiency: up to ~80% of this transmitted energy can be captured by the working fluid of a CCGT [4]. High temperatures, ranging from 900 to 1500 °C, are thereby achievable in practice [9]. A compressor, energised by the working fluid of a CCGT, operating in tandem with such a concentrator, has pressurised air (or another gas) from 1 Bar up to approximately 35 Bar and hence achieved pressure-ratios that can enable a CCGT to operate with an 80% efficiency. Table 2 shows the operating characteristics, under both test and simulated conditions, of a combined 30 kW solar-energy concentrator and CCGT system.

The salient features of Tables 1 and 2, with regard to CHP and CPP (e.g. for > 1 MW gas-turbine engines), are the high values of both the exhaust mass-flow and the exhaust temperature. Hence, rapid transfers of high-grade heat, e.g. at ~600 °C, from the primary-generator's exhaust to act as the input for a secondary generator of electricity are feasible [10].

Using a solar mirror concentrator with a minimum area of 200 m^2, a CCGT with an 18:1 (or greater) pressure-ratio and an inlet-to-outlet temperature-drop ranging from 1200 to 600 °C can easily be stimulated to provide a sufficiently-worthwhile power output. The waste-heat output from such a system should be sufficient to drive a steam turbine or several pure-reaction, impulse turbines. Hence a solar-powered Brayton/Rankine cycle could be employed, in principle, with an organic Rankine cycle forming the third-stage (bottoming) power-cycle.

Using a magnetohydrodynamic (MHD) topping-cycle [9], fossil-fuel exhaust gases can be ionised as they pass between magnets so that an electric current flows between a pair of electrodes, which are set orthogonal to the parallel magnet-faces. Net efficiencies of 60% are predicted for such a magnetohydrodynamic/Brayton/Rankine cycle [9]. In southern Britain, with an average daily solar irradiation duration of ~5 h [11], such a system would not at present be economically viable because appropriate inexpensive large-area mirror-systems are not available. However, in the tropics, where countries receive far larger amounts of insolation daily, and where cheap labour and surplus aluminium are readily available (as in Brazil, e.g. for the construction of parabolic mirrors), a CPP plant combined with a hydroelectric storage system may eventually become commercially worthwhile. A composite electricity-generator, that utilises other local sources of energy, e.g. wind-power, photovoltaic electricity and/or fossil fuels, would be attractive, especially if the combined output of the integrated system could remain approximately constant, even though the percentage energy contributions from the individual components vary.

The conversion of solar thermal-energy directly to electricity (without the use of a compressor and turbine system) is now commonplace: in AD 1984, a world record of 30% efficiency was achieved for the direct conversion of sunlight to electricity [12]. [The effectiveness of a solar-energy harnessing system is appropriately higher if it captures both direct and reflected (e.g. from a sea surface) insolations]. A

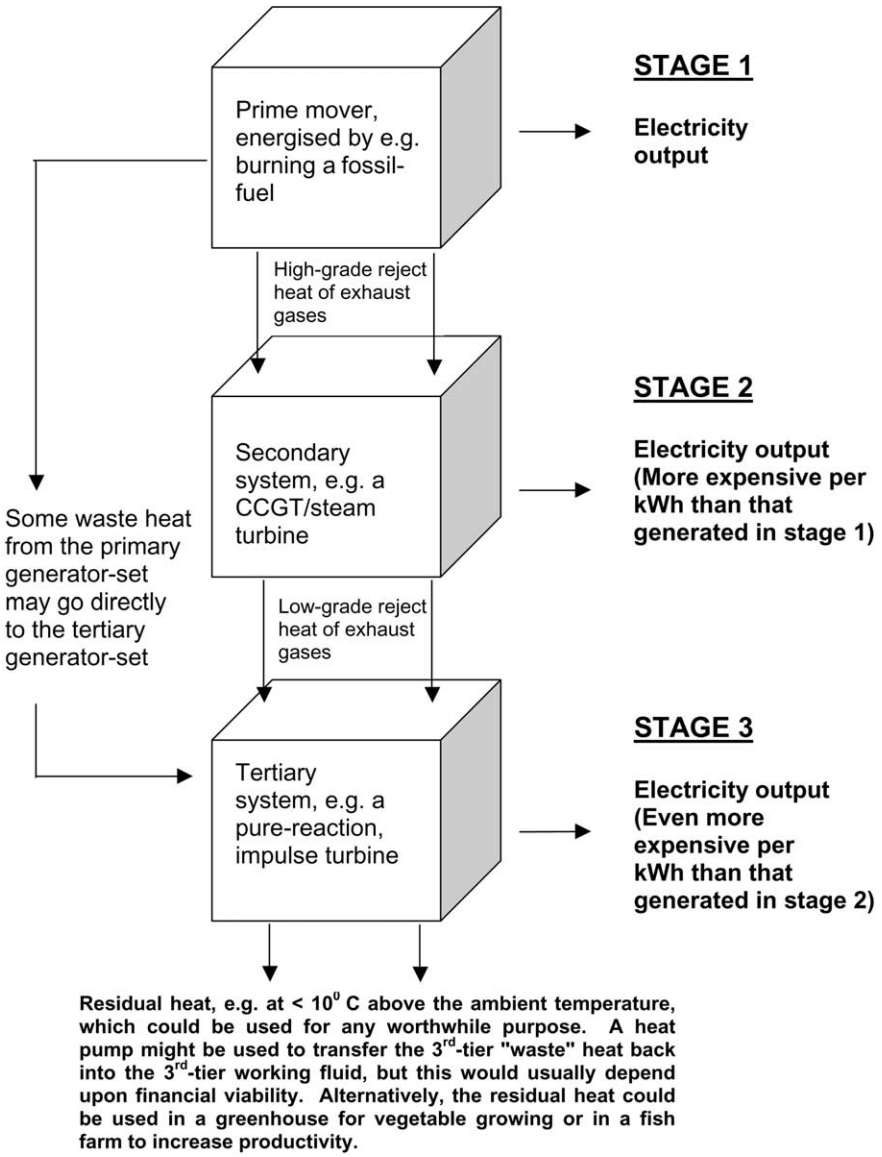

Fig. 1. Schematic diagram of the proposed cascaded sequence of primary, secondary and tertiary generators of electricity, i.e. the integrated CPP generator.

compound generator, with insolation from a 10.3 m compound parabolic mirror energised a Stirling engine: it heated 7 g of hydrogen at a pressure of 15 MPa, to 1073 K, with about half the energy produced being absorbed by the cooling water [13].

Commercially-available, parabolic-mirror systems can achieve concentrations that range up to 1000:1, whereas concentrations for trough heaters are less than 50:1 [12].

Table 1
Typical characteristics of various types of prime-mover that are used for electricity generation (after Rameau[3])

Prime-mover	Spark-ignition engine	'Diesel' engine	OCGT	CCGT	Back-pressure steam-turbine[a]	Pass-out steam-turbine[a]
Fuel used	Natural gas or biogas	Natural gas, biogas, gas oil or heavy fuel-oil	Natural gas, biogas or gas oil	Natural gas, biogas or gas oil	Any fuel	Any fuel
Power output	15 kW_e–2 MW_e	30 kW_e–6 MW_e	$\geqslant$1MW_e	$\geqslant$3 MW_e	$\geqslant$500 kW_e	$\geqslant$1 MW_e
Thermal-to-electrical power outputs	1:1–2:1	1:1–1.5:1, or up to 5:1 with boost firing	1:1–3:1, or up to 5:1 with supplementary firing	1:1, or up to 3:1 with supplementary firing	3:1–>10:1	3:1–>8:1
Heat output	LPHW[b] or steam	LPHW or steam	High-grade steam	Medium-grade steam	Medium-grade steam	Steam at ~2 atm
Electricity-generating efficiency (%)	25–35	35–45	20–40	35–50	7–20	10–20
Overall efficiency when "waste" heat is usefully employed (%)	70–78	65–75 or up to 82 with boost firing	65–80 or up to 82 with supplementary firing	73–80 or up to 85 with supplementary firing	75–84[a]	75–84[a]
Capital cost (£/kWh output)	550–580	500–800	500–1500	500–700	600–2000	600–2000
Operation and maintenance cost (p/kW)	0.5–0.8	0.4–0.8	0.2–0.7	0.2–0.7	~0.1	~0.1

[a] Efficiency of a steam-turbine is very dependent on its size.
[b] LPHW low-pressure hot-water.

Table 2
Typical intake requirements and output characteristics for a 30 kW commercially-viable solar-energy concentrator and (a computer simulation of the performance of) a theoretical CCGT system, undertaken at the Weizmann Institute [4]

Solar-concentrator receiver: June 23, 1996, in the Negev Desert	Recorded insolation on local ground ($W\ m^{-2}$)	Concentration ratio	Concentrator's photon loss (%)	Air-inlet temperature (K)	Air-outlet temperature (K)	Receiver's efficiency (%)
	~870	~10,000:1	~1	308	1204	79
CCGT (in series with the concentrator)	Receiver output (kW)	Working pressure (Bar)	Air mass flow rate ($kg\ s^{-1}$)	Turbine's air-inlet temperature (K)	Turbine's air-outlet temperature (K)	Net efficiency (%)
	30	18	0.022	~1200	~600	20

One reason that parabolic mirrors have not become more popular is that their harnessing efficiencies decrease as the temperature rises due to the resulting physical distortions of the mirror surfaces. However, with a Carnot-cycle Stirling engine, the efficiency increases as the maximum temperature of the working-fluid increases. Thus an optimal working-fluid temperature, in the range of 400–800 °C, should be employed.

A 10.3-m diameter composite-mirror dish, i.e. composed of smaller mirror units that can achieve a concentration leading to the attainment of a working-fluid temperature of 800 °C and deliver 30 kW of electricity to the grid, cost US $4,000,000 at 1984 prices [12], e.g. ~£10 per kWh at 2002 prices, i.e. highly expensive!

The unit fossil-fuel costs for the engines in Table 1 will probably inflate rapidly after 2020 AD [14,15] and so renewable sources, of for instance hydroelectric power or solar energy, will be employed increasingly. The recent introduction of heliostats, e.g. primary parabolic and secondary hyperbolic mirrors combined with insolation concentrators, has led to the conclusion that multiple solar energy-CCGT steam-turbine generator-sets and methane reformer-sets (that deliver ~178 GWh annually) could provide a partial solution to the problem of fossil-fuel reserves depletion [9]. For example, most (~79%) of the solar energy, absorbed by a working 30 kW solar receiver (Table 2, row 2) can be absorbed directly by the compressed air formed when a CCGT compressor pressurises the working-fluid, i.e. air, from 1 to 18 Bar [9]; the waste-heat being used to drive a steam turbine.

Due to aberrations and thermal strains in the mirror surface (i.e. the dish) and attenuation of the insolation in the Earth's atmosphere, working parabolic mirrors have a maximum theoretically-achievable power-concentration limit of ~10,000:1. Fig. 2 shows that the maximum concentration occurs with a rim-angle (half-angle) of 45° for a single parabolic mirror.

Fig. 2 depicts the concentration maximum that could be achieved with aluminium parabolic mirrors, i.e. heliostats. Secondary lenses can be added to the system in

order to concentrate the insolation further, but this would be unlikely to be cost effective.

A secondary concentrator (to achieve even greater insolation intensities) might be a further secondary parabolic-receiver or a lens-mirror concentrating-system, but the cost effectiveness of these additions at present is doubtful. Fig. 3a and b depict a proposed secondary solar-energy concentrator/receiver-system.

Feasibility studies are currently underway concerning the design and construction of large-scale NIR reflecting towers (RSTs), e.g. by the Weizmann Institute [9]—see Fig. 4.

4. Secondary-generation prospects

The heat rejected, with a primary-generator's flue-gases or from the generator's condenser or the cylinder's cooling system, can be used as a heat input to a low-grade-energy system for generating electricity. It can also be supplemented by the residual heat arising from the primary-stage compressor's waste-heat as well as, for instance, by any available harnessed renewable energy.

A reaction turbine, with an inlet temperature of approximately 873 K and a temperature drop of ~330 °C, could be driven continuously using energy from the exhaust heat of the CCGT or OCGT unit mentioned in Table 1. A typical multi-stage steam-turbine, can be employed with large working-fluid mass flows. Alternatively, for working-fluid flows of less than 1 kg s^{-1}, either a once-through impulse turbine, a bespoke-designed reaction turbine or a combination of these two, could be used as the secondary generator [16,17]. Fig. 5 provides design guidance as to which steam-turbine type to adopt (for mass flows of less than 1 kg s^{-1}).

An alternative to an impulse or reaction turbine is a single-stage radial-flow turbine, followed by a multi-stage axial-flow reaction turbine [17]; for the latter, the efficiencies per stage range from 0.75 to 0.95. For a single-stage radial flow, followed by a 5-stage axial-flow reaction turbine, the overall efficiency can range from 0.18 to 0.74.

Rankine-cycle (see Fig. 6) waste-heat from the secondary generation system could provide the heat input for a tertiary-stage generation, but the economics of the latter are usually unattractive.

Table 3 provides the mass flow, mean temperature and average specific-heat of the exhaust gases from the primary generator to be used as input data for the secondary generator. Then the Mollier diagram for steam allows us to choose the reasonable value for the secondary-turbine's initial inlet pressure of 2.3 Bar and corresponding inlet temperature of 863 K [19]. This decision enables the designer to achieve a reasonable inlet-to-outlet pressure-ratio, i.e. 18:1, and an outlet temperature that is well-above the saturation temperature, i.e. 260 °C. We thus have a dry working-fluid for the secondary generator throughout all its turbine stages [20,21].

A tropical ambient temperature can be as high as 313 K. The condenser temperature might be ~10 °C above this, allowing for a normal temperature-difference of approximately 10 °C between the cold sink and the working fluid. This will

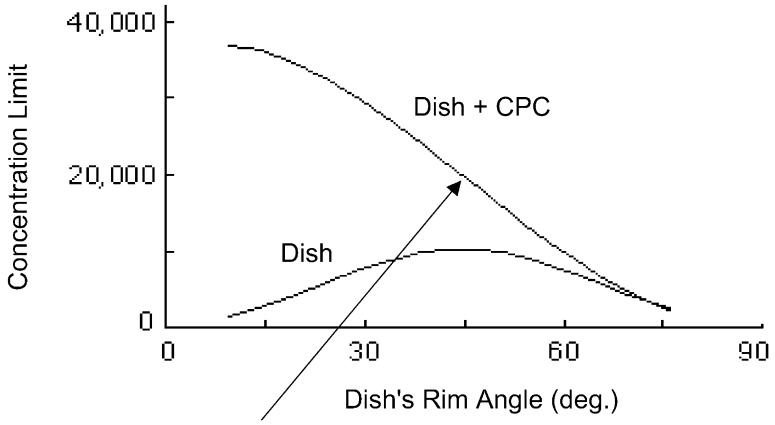

Fig. 2. The lower curve shows the near-infrared (NIR) solar-energy concentration for an aluminium parabolic dish. (The dish's rim-angle is that formed by the mirror's axis and a line drawn from the centre of the mirror to the mirror rim.) The upper curve shows the theoretical concentration limit for a two-stage NIR solar-energy concentration system, with a parabolic– dish primary-mirror and a compound parabolic-concentrator secondary mirror, as a function of the dish's rim-angle. The arrow indicates a significant increase of insolation concentration when the secondary concentration system receives the output from a 45° rim-angle parabolic-mirror (after Kribus [18]).

correspond to an initial pressure-ratio of 2.3:0.125, i.e. 18:1, because the steam condenser pressure at 323 K is approximately 0.125 Bar [22].

It may be economically justifiable to use the primary-turbine's waste-heat as the secondary-generator's input heat (see Fig. 1). For the assumed conditions, the primary-unit's exhaust can leave the gas turbine at a maximum of 873 K. This is near the maximum for a steam-turbine's inlet temperature, so close matching can be achieved.

The theoretically-predicted power-output of 720 kW (see Table 3) will be reduced in practice because of the thermal resistances to heat transfers, gearing losses and generator inefficiencies. Reasonable values of the respective coefficients for these parameters are 0.90 each for the two heat-exchangers, 0.98 for the gearing dissipation, and 0.95 for the generator losses [23]. Hence the realistic electrical output power for the reaction turbine (as described by the performance data in Table 3) would be $720(0.9)^2(0.98)(0.95)$, i.e. 542.9 kW. So, in practice, one might expect $\sim$500 kW per kg s^{-1} of working fluid. Larger working-liquid mass flows, i.e. greater than 1 kg s^{-1}, will be able to drive a high-efficiency reaction steam-turbine, whereas, for smaller mass flows, a once-through impulse turbine or a compound impulse/reaction turbine would be more appropriate. However, only relatively low efficiencies are achieved with either of the latter two designs and so 200–250 kW specific power outputs would probably be more realistic expectations rather than those near 500 kW [16]. With high efficiency ($\sim$0.85) first-stage modern CCGTs, tertiary generation of electricity will probably never be viable economically. Nevertheless, it's potential needs to be assessed.

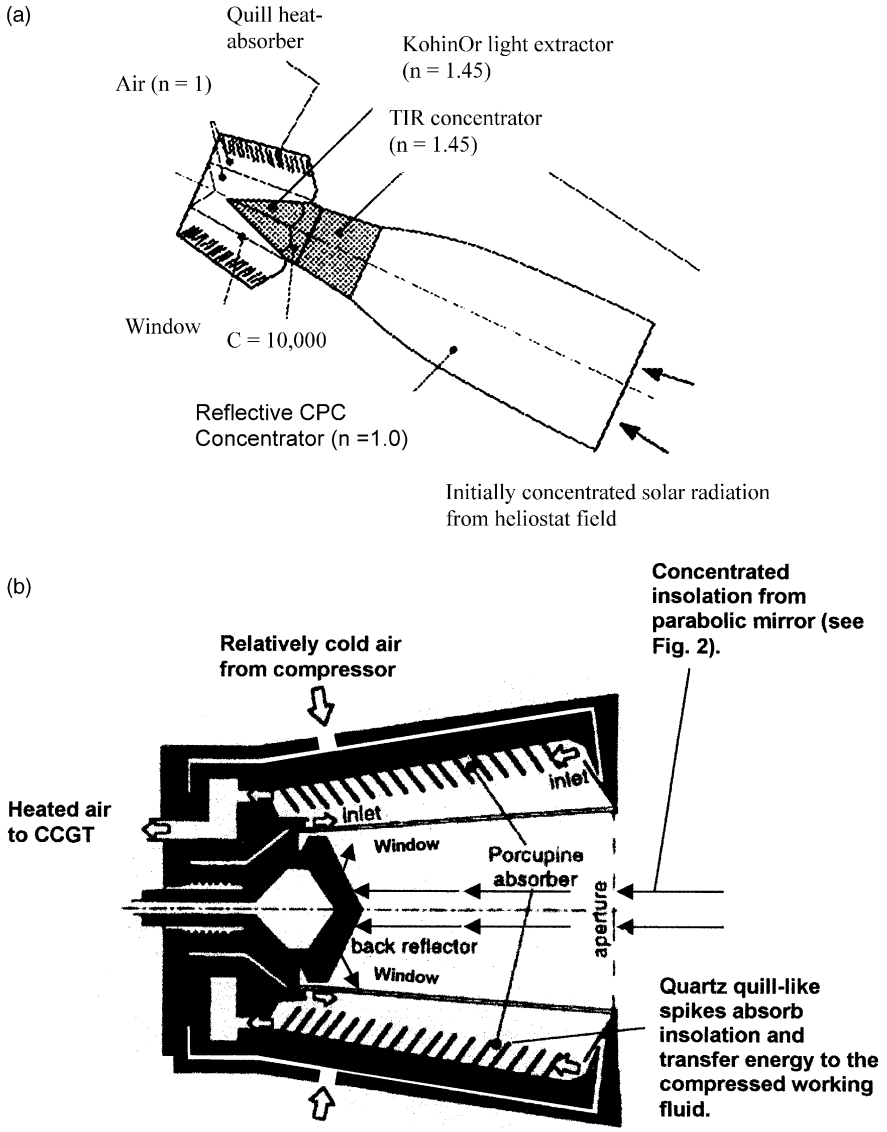

Fig. 3. (a) The secondary CPC with further details of the insolation absorber provided in Fig. 3b [4]. (b). A schematic radial section of the proposed insolation receiver. Black arrows depict incoming-concentrated insolation from a parabolic mirror as well as internally-reflected insolation. An auxiliary compressor pumps in air at 20 Bar. As it slows over the porcupine-like quartz quills, air heats up to approximately 1500 K. It then leaves the concentration and passes into a CCGT [4].

5. Tertiary-generation prospects

A prospective choice of working fluid to handle the 'waste' heat-output from the systems proposed earlier is ethanol [24–25]—see Table 4. Ethanol's critical temperature is

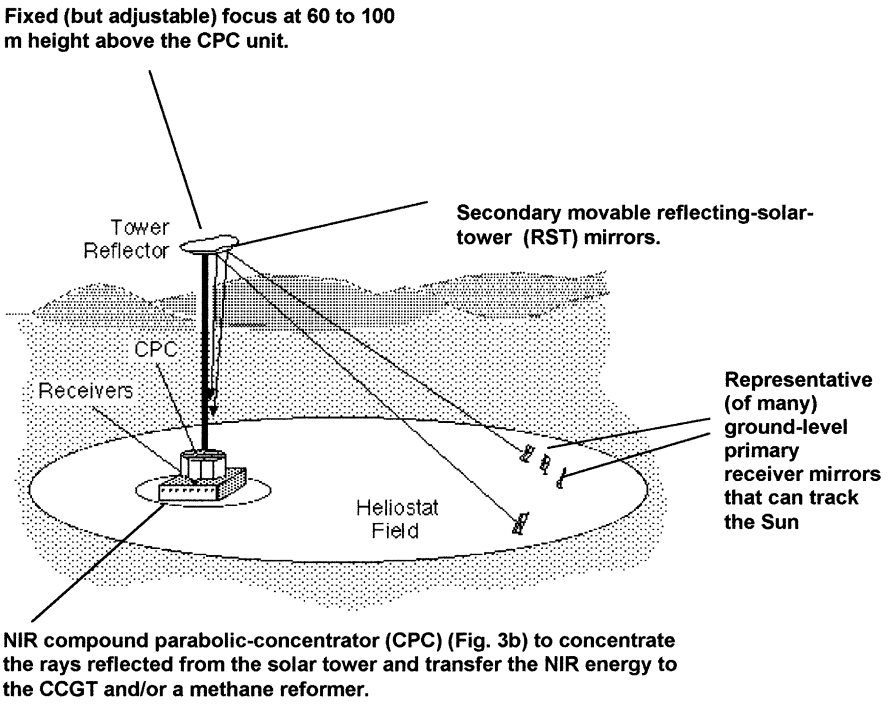

Fig. 4. A working NIR RST.

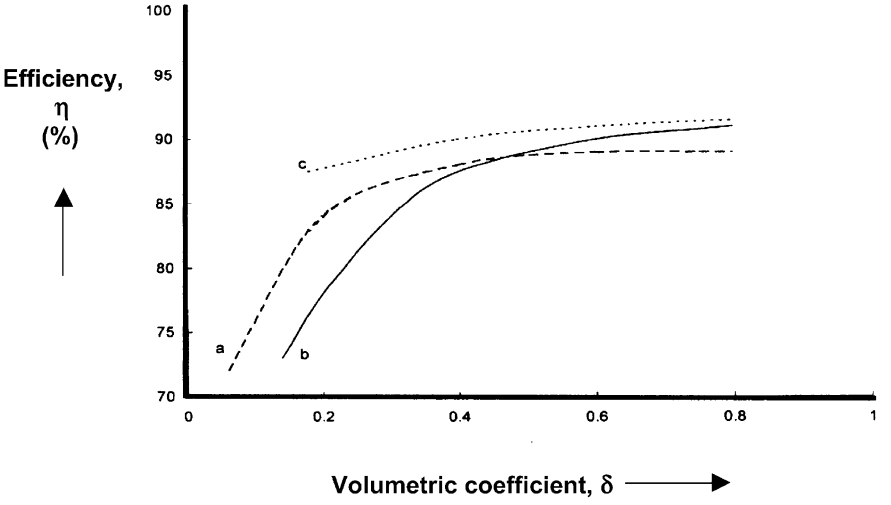

Fig. 5. Efficiencies of representative impulse and reaction turbines [18]. a, Impulse turbine; b, reaction turbine; c, reaction turbine with shrouding.

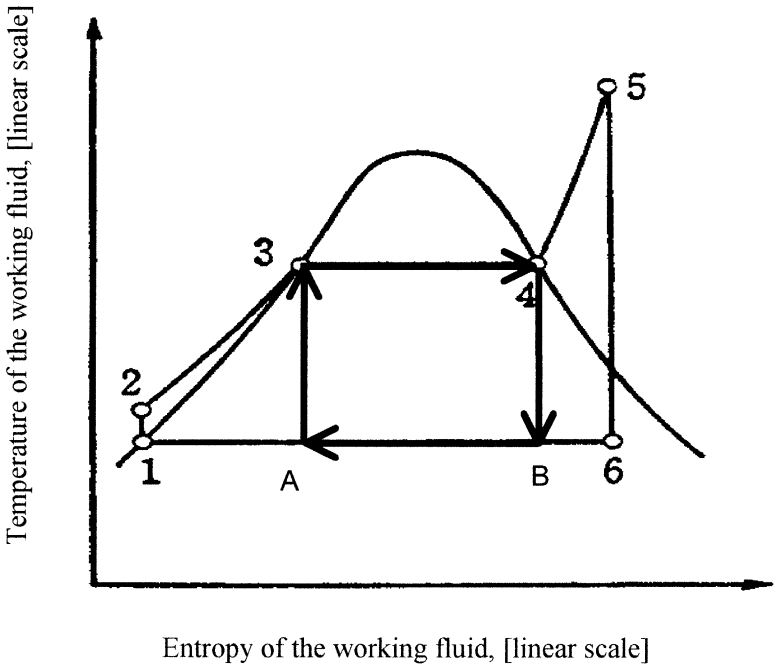

Fig. 6. Rankine cycle (stages 1→2→3→4→5→6→1) for secondary generation and corresponding Carnot cycle (stages A→3→4→B→A) [10]. Rankine-cycle processes: 1→ 2, working fluid is pumped to boiler; 2→ 3, boiler heats the working fluid to its boiling point; 3→ 4, working-fluid boils; 4→ 5 , the generated vapour is superheated; 5→ 6, superheated vapour does work; 6→ 1, the vapour is condensed (so releasing heat to stimulate the tertiary system's boiler).

Table 3
Data for the secondary-generator's reaction-turbine

Inlet pressure	2.3 Bar
Inlet temperature	863 K
Outlet pressure	0.125 Bar
Condenser temperature	323 K
Outlet temperature	533 K (accounting for entropy losses)
Mass flow, $\dot{m}$, of working fluid	$\leqslant 1$ kg s^{-1}
Superheat possible	465 °C, i.e. from 398 to 863 K
Isentropic enthalpy drop	$\sim$900 kJ kg^{-1}
Assumed efficiency of 2nd stage	0.8
Real enthalpy drop	720 kJ kg^{-1} (accounting for entropy losses)
Specific work output	720 kJ kg^{-1} (accounting for entropy losses)
Power output	720 kW (for $\dot{m} = 1$ kg s^{-1})

The gross power output of the theoretical reaction-turbine (i.e. the secondary generator) is deduced for the situation when the CCGT's (i.e. the primary generator's) exhaust-gases are used to heat water, and the superheated steam so produced provides the input energy for the secondary generator [19].

516 K, which is slightly less than the secondary generator turbine's outlet-temperature of 533 K (see Table 3) and hence nearer the working source temperature, i.e. 10 °C less than 533 K [28].

Ethanol has two absorption bands, at approximately 3 and 9.5 microns wavelengths [29], which can be stimulated by the emissions respectively of a relatively inexpensive microwave semi-conductor laser and a more expensive CO_2-gas laser [30]. A working fluid may have different absorption wavebands for its liquid and vapour states. This difference may allow useful stimulation of the working fluid by different heat sources, e.g. two different-wavelength laser outputs. For example, liquid ethanol can be vaporised totally by the 3-micron emission and then the vapour may be superheated (if necessary) by the 9.5 micron emission. This means that a totally dry vapour can be obtained from a laser-modulated working-fluid just above its saturation temperature and then superheated with a secondary (but, currently highly expensive CO_2) laser. This process has other useful applications. Because liquid water absorbs radiation at 3 microns, a microwave laser embedded in the stator of the last few stages of a reaction turbine could prevent condensation (and hence inhibit erosion) of the turbine blades. This could be achieved at relatively low cost with a semiconductor-microwave laser to provide dry steam.

It is feasible to obtain sufficient energy to perform this function (i.e. for driving the tertiary-system's turbine). The economic viability of the process would be determined by consideration of the laser system's cost and that for replacing any eroded turbine blades. However, the commercial superheating of ethanol vapour by means of CO_2-laser emission will have to await the development of an inexpensive 9.5 micron wavelength output semi-conductor laser.

Two-phase flow can be studied via a set of equations describing the total energy obtainable from the two-phase flow as the sum of the kinetic energies of the vapour and the liquid fractions [31,32]. The maximum kinetic energy of a two-phase flow has been estimated to occur when the vapour fraction occupies approximately 70% of the working-fluids volume [32–34].

From Table 3, it can be seen that the working-fluid's temperature during operation will be less than 170 °C above its saturation temperature and therefore the working-fluid is in the form of a wet vapour, so posing erosion problems [35,36]. One possibility in these circumstances, would be to make use of a two-phase flow to drive a compound pure-reaction, impulse turbine [37,38]. Fig. 7 shows a boiler system for producing such a two-phase flow. Included in the prototype design are options such as an acoustic transducer, which could be used to measure flow rates and a laser to detect the type of flow regime present. [The use of a laser in the measurement system has an additional

Table 4
Thermodynamic properties of ethanol [26–27]

Temperature of boiling	Specific liquid volume ($m^3\ kg^{-1}$)	Liquid density ($kg\ m^{-3}$)	Specific volume of vapour ($m^3\ kg^{-1}$)	Specific heat of evaporation ($kJ\ kg^{-1}$)
351.5 K @≈1 Bar	0.00132	757.08	0.7265	960
323.0 K @≈0.294 Bar	0.00128	782.22	0.4417	982

benefit. If the laser emission wavelength lies within the working-fluid's absorption band, then the laser output becomes an additional, though relatively small, heat source for the third stage. However, for this application, the use of a laser for producing heat as its prime purpose would be excessively expensive. Nevertheless, the working fluid being pumped (see component 15 in Fig. 7) from the condenser to the boiler, can capture some of the wild heat generated by the laser and usefully employ it in the tertiary generator.]

A low-grade-energy input generator for electricity generation, e.g. see Fig. 7, should use available waste-heat from previous generator stages and any harnessed renewable energy. This tertiary generator's efficiency will be influenced by the temperature of the environment immediately surrounding the generator, which consequently should be in a well thermally-insulated enclosure. The energy-input rate to stimulate the two-phase flow turbine should be high enough to evaporate a significant proportion of the working fluid. If a pressure-ratio of approximately 3:1 can be achieved, enough torque will be generated to make its use worthwhile [35].

Table 5 provides details of the possible output values achievable for given input values, i.e. with a pure-reaction, impulse turbine as in Fig. 7.

Any rotating device will produce vibrations within it at certain frequencies. Fig. 8 depicts how a turbine's vibrational energy might also be used to produce an electric current, but, in practice, this is likely to be uneconomic.

With regard to Fig. 8, when a permanent magnet moves in the upward direction (as indicated by the upward-pointing arrows), the current moves in the same direction within the counter-clockwise wound coil 2. Coil 1 is part of an open circuit in this (first) half-cycle due to a transistor switch system [39,40].

The next step, i.e. step 2, occurs when a permanent magnet moves in a downward direction: then the current moves in the opposite direction within the clockwise-wound coil 1. Coil 2 is then in an open circuit in this (second) half-cycle due to a transistor-switch system. The two half-cycles thus result in two forward DC pulses in the transformer. The permanent magnets' electrical-output can now enter coil 3, or a winding around the soft-iron electromagnet (not shown). A controllable force field will now exist on opposite sides of the machine.

When a soft (pure iron) electromagnet is employed as the (lower) magnet in Fig. 8, and moves in the upward direction indicated by the arrow, the current moves in the opposite direction, i.e. in the clockwise-wound coil 3. Coil 1 is in an open circuit in this (first) half-cycle. Coil 2 then produces a voltage in the transformer [41]. This voltage causes an output current to flow in the transformer output, which can now enter coil 3. The current flow in coil 3 will create a magnetic force-field [42]. Coil 3's magnetic force field then opposes the electromagnet's force-field and dampens the engine-block vibration or permits a stable frequency of vibration to be achieved.

6. How much power can a two-phase flow transfer?

A two-phase flow pure-reaction impulse turbine [43] could remove 800 kW of low-grade energy, e.g. waste-heat at 120–300 °C, and convert it into useful electricity (Fig. 7 and Table 4). The derisory electrical output may be only ~2 kW, but this is

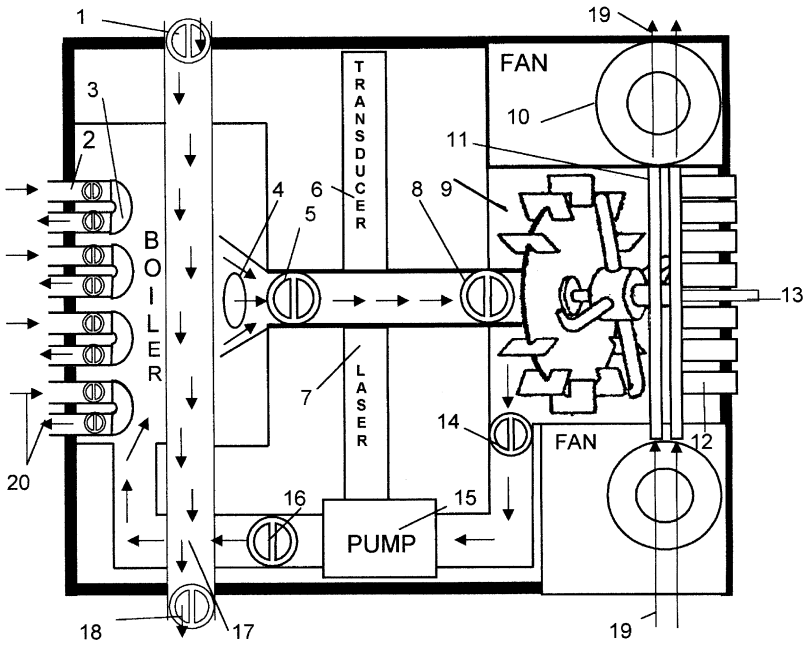

1. Inlet pipe and valve for hot flue gases from primary and secondary generators
2. Inlet pipes and valves for hot coolant from primary and secondary generators
3. Liquid-to-liquid heat-exchanger
4. Electric-coil heating element (output-energised to stabilise flow)
5. Two-phase flow pipe's inlet-valve
6. Acoustic transducer to measure flow for stabilisation purposes
7. Laser measurement system determines flow regime: could also provide a little additional heat
8. Two-phase flow pipe's outlet-valve
9. Pure-reaction turbine arms and impulse-turbine plates
10. Inlet/outlet cooling fans (optional)
11. Fan's heat-exchanger cooling pipes
12. Heat pipes from condenser to another (optional) energy converter
13. Generator axle
14. Condenser's flow exit-valve
15. Condenser's feed-pump returns liquid to boiler: liquid could also cool the laser
16. Boiler-flow admission valve, used to stabilise the boiler flow and pressure
17. Gas-to-liquid heat-exchanger
18. Gas heat-exchanger's exit-valve
19. Flow direction of cooling-fan air
20. Flow direction of hot coolant from the primary and secondary generators into, and out from, the tertiary boiler

Fig. 7. Schematic design of a possible third-stage two-phase flow energy-converter of a cascaded electricity-generation system.

the average per capita power requirement in the UK [44]. Ancillary output power from vibrations may also be used to help dampen potentially harmful harmonic vibrations by converting the energy of the mechanical vibrations into electrical and then electromagnetic energy (see Fig. 8).

The energy conversion efficiency of a pure-reaction, impulse turbine is low (Fig. 7, Table 4), and the temperature of the "waste" heat output may be $<10\ ^{\circ}C$ above the ambient temperature. Nevertheless, this residual low-grade heat may be transformed by a heat pump into a more useful higher-grade heat [45], which the ethanol in the pure-reaction, impulse turbine may be able to absorb (see Fig. 7, [46]). The heat pipes (component 12 in Fig. 7) enable the system to function without the use of

Table 5
Typical thermodynamic parameters and output characteristics for a pure-reaction, impulse turbine for the tertiary generator using ethanol as the working fluid

Mass flow (kg s^{-1})	Inlet temperature of heat sources (K)	Boiler temperature (K)	Condenser temperature (K)	Boiler pressure (Bar)	Condenser pressure (Bar)	Power (kW)
10.0	373–573	351	323	1.00	0.29	2.00

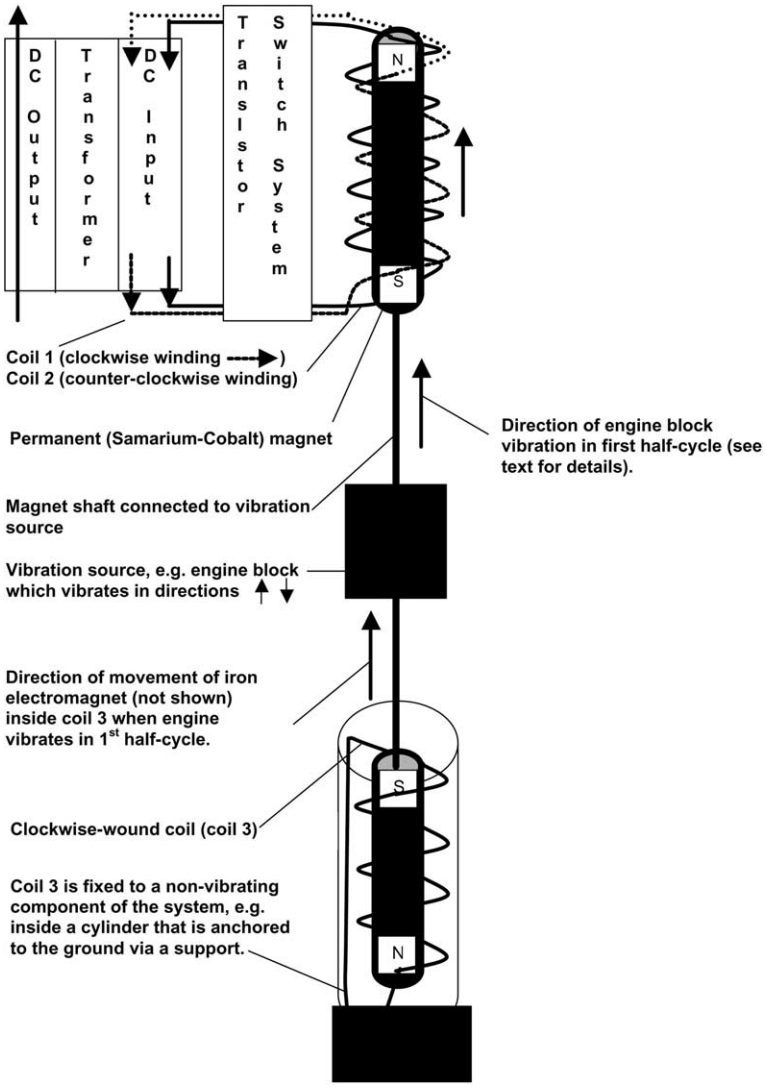

Fig. 8. An electro-mechanical system that converts mechanical vibrations to a DC pulsed current.

power-consuming electric fans. The waste-heat from the pure-reaction, impulse turbine can be used as the input to a second turbine.

Alternatively, a new design (see Fig. 9) could be employed: this would involve the insertion of a turbine-driven dynamo unit into a heat pipe, in order to aid the action of the condenser (see component 12 in Fig. 7). This unit might employ directly the power output from a parabolic solar-energy collector. In an appropriately-designed heat-pipe, the pressure at the evaporator end could be significantly higher than at the condenser end, e.g. a pressure difference of 1 Bar may exist [45]. This is equivalent to the pressure difference in some engines, e.g. a multi-vane expander [35].

Fig. 9a and b depict a heat pipe with a turbine inserted in the evaporator section. In this form of heat-pipe, the returning liquid in the outer wick's return-passage is shielded from the upward-moving vapour by a glass cylinder. Heat pipes with separate returning-liquid paths and vapour paths have been employed before, e.g. in a NASA thermally-controlled spacesuit [51]. However a centrally-placed glass cylinder has been inserted to prevent interference between the returning liquid and the upward-moving vapour. Fig. 10 indicates the factors that limit the rate of heat transfer through a heat pipe as the source temperature is raised, i.e. from the working-fluid's boiling temperature to its maximum working limit, while the condenser end is maintained at a constant temperature. Section 1–2 is with the source temperature, at or just above, the working-fluid's boiling-point: the rate of heat transfer is limited by the velocity of sound in the working-fluid vapour at the given temperature and the pressure. Section 2–3 depicts that, with a slightly higher source-temperature, the limiting factor is the entrainment of the returning working-liquid by the outgoing vapour: the centrally-inserted glass-section in Fig. 9a would avoid this entrainment. With a further increase in source temperature, i.e. Section 3–4, the limiting factor becomes the ability of the heat-pipe to return the working-liquid via the wick. Section 4–5 depicts that, at an even higher source temperature, complete boiling of the working-liquid ensures there is insufficient returning liquid.

A small turbine connected to two powerful Tesla Samarium-Cobalt magnets could be a generator of electricity, described by

$$V = \frac{B\dot{\theta}NA}{2} \tag{1}$$

where the V is the voltage generated; B the strength of the magnet; $\dot{\theta}$ the dynamo-axle's rotational frequency, N the number of magnet poles that face the coil windings; and A the area of one pole face of one magnet [41].

The heat-pipe turbine might be described as a one-stage impulse turbine. So, in order to obtain a first approximation, the basic shaft-power Eq. (2) is used to estimate the maximum theoretically-possible electric-power output [52]: in reality, it would be significantly less.

$$\text{Shaft Work} = (\text{Mass flow rate})\eta C_P T_2\left[\left\{p_1/p_2\right\}^{R/C_p} - 1\right] \tag{2}$$

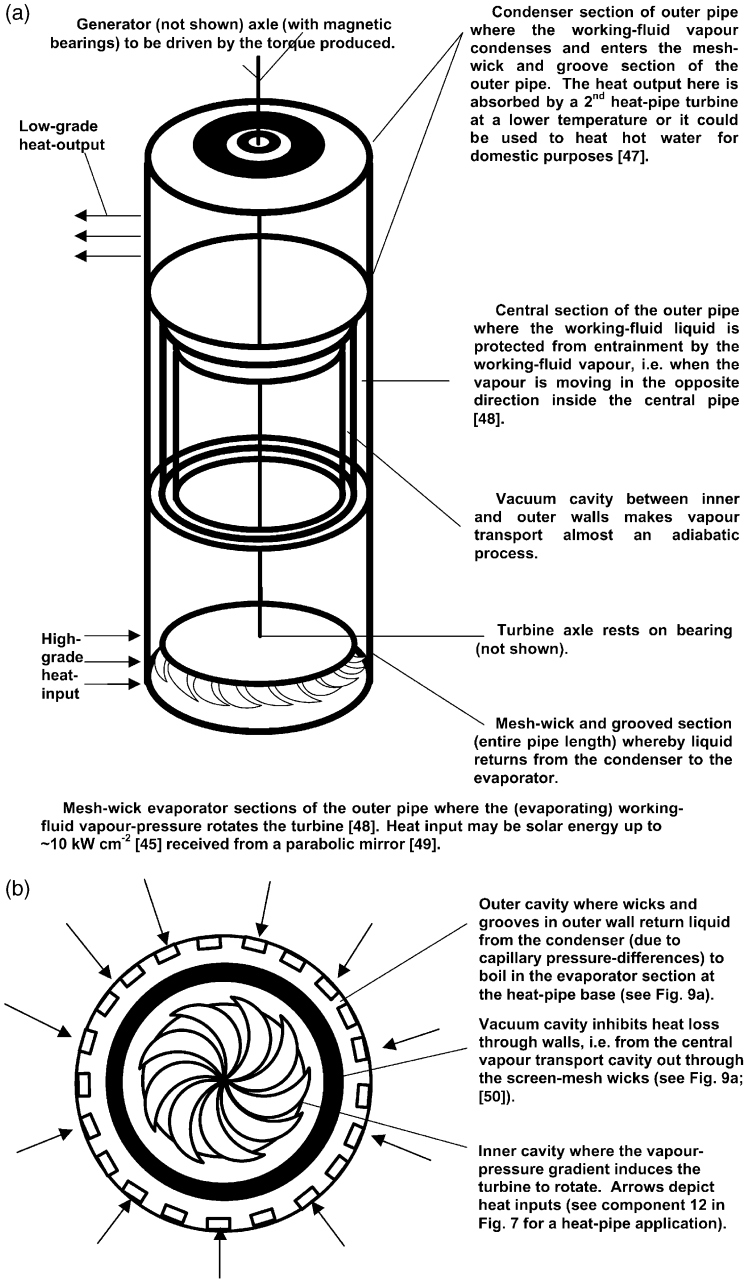

Fig. 9. (a) Schematic foreshortened version of the heat pipe with insulated central section. Upper 3 arrows depict low-grade heat output. Lower 3 arrows depict high-grade heat input, e.g. from secondary generator's "waste" heat [45,47–50]. (b) Plan view of the base of the heat-pipe shown in Fig. 9a [71].

where η is the efficiency; C_P the specific heat capacity of the working fluid, i.e. 2100 J kg^{-1} K^{-1} for steam; T_2 the heat-pipe's condenser temperature; p_1 the evaporator pressure; p_2 the condenser pressure; and R is the gas constant for H_2O, i.e. 461.5 J kg^{-1} K^{-1} [22].

Using water as the working fluid, assuming a mass flow rate of 4.42×10^{-4} kg s^{-1} (due to an insolation of 2 kW on a 2 m^2 collector, with a NIR power content of 1 kW), a maximum efficiency of 0.8, a condenser temperature of 323 K and Eq. (2), the maximum gross power output would be 139 W from 2 kW of insolation [52], as may be seen from

$$(4.43 \times 10^{-4})0.8(2100)323\left[\{1.00/0.125\}^{461.5/2100}-1\right] = 139\text{W}$$

A net output of electrical power of approximately 100 W is then theoretically possible.

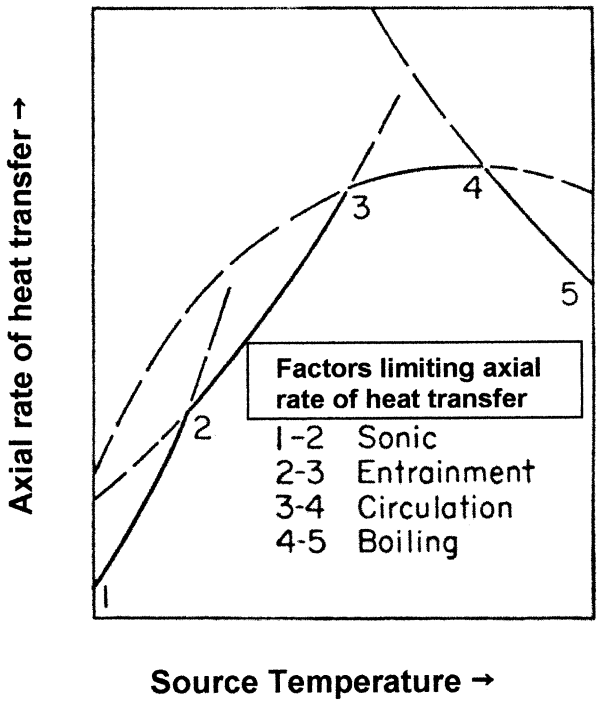

Fig. 10. Heat-pipe's operating envelope, e.g. any point on the numbered solid-line sections depicts the maximum axial rate of heat transfer at the specified source temperature. The maximum rate is limited by:- the speed of sound in the working-fluid gas (1–2); entrainment of liquid by gas flow in the opposite direction (2–3); the liquid return flow in the wick (3–4); and overheating in the evaporator (4–5) [45].

7. How to increase electricity generation from solar power using a composite system

In 1929, a Finnish inventor, Sigurd J. Savonius, patented a vertical- axis wind-turbine, which has subsequently been referred to as the Savonius rotor. He noted that rotating vertical partial cylindrical blades could harness up to 31% of the wind's energy from the swept area [53,54].

The advantages of a vertical-axis wind turbine compared with a near-horizontal-axis turbine are that the vertical-axis turbine is not limited with respect to any particular wind direction and it is relatively quiet running. However vertical-axis machines have a high starting-torque and the power output varies approximately with the square of wind velocity, whereas that for a horizontal-axis turbine is proportional to a somewhat higher power of wind speed. The outer surfaces, i.e. the blades, could be covered with a coating of photovoltaic silicon in order to capture solar energy. The vertical support could be made hollow in order to facilitate the pumping of water up to a reservoir, placed above the entire rotor system. These are possibilities for future exploitation when the economics are more favourable.

8. Energy storage and subsequent electric-power generation using a water reservoir

Energy produced from a fluctuating power source, such as that harnessed from the Sun, may be stored in order to be used later (e.g. at night). Water is a good, safe, inexpensive working-fluid that may be used to store potential energy, i.e. at a height, or as steam under pressure.

The maximum power obtainable from the potential energy of water stored at a height, h, is

$$W = \rho g h \dot{V} \tag{3}$$

Eq. (3) states that the product of the liquid working-fluid's density ρ, its acceleration g due to the Earth's gravity, the reservoir's water-surface height h above the turbine and the water's volumetric rate $\dot{V}$ of flow equals the maximum theoretical output power of the turbine.

Assuming a pumping efficiency of $\sim$80% and a combined water-turbine generator efficiency of $\sim$75% [55], then $\sim$60% of any excess electricity supply could be re-supplied by this system at a later time, e.g. overnight when there is no solar power available, if water is pumped up to the reservoir during the previous day. For example, a volumetric flow of water of $\sim$20 $m^3\ s^{-1}$ at a height of 100 m would give a gross output power of $\sim$20 MW. By using the earlier-mentioned efficiency figure of 75%, approximately 15 MW_e of electrical power could be generated for a period dependent upon the capacity of the water-tower or reservoir. If the total efficiency of the system is $\sim$60%, then a power consumption of 25 MW would be required to pump the ground water up to the water reservoir from where it can be subsequently extracted to do useful work.

If this power were to be derived from solar photovoltaic energy, i.e. assuming a 25% efficiency for the photovoltaic cells and an insolation of 1000 W m^{-2}, then normally a minimum of approximately 100,000 m^2 of PV cells would be required. By using both the potential photovoltaic and NIR energies of the solar spectrum, this figure may be reduced significantly.

A combined RST-water tower covered with a layer of photovoltaic cells and configured with aerodynamically-sculpted blades on a centrally-positioned Savonius rotor, e.g. on the water reservoir's vertical pipe section (see Figs. 4 and 11), might be a worthwhile incremental innovation to existing designs [57].

For example, a 100 m high water-surface reservoir pipe with a 10 m diameter would have a total useful surface area of ~3,000 m^2. Combining this area with an upper spherical water reservoir of approximately 25 m radius would provide a total useful surface area of ~10,000 m^2, e.g. 10% of the earlier estimated minimum required value of 100,000 m^2. Therefore a ground-based array of solar photovoltaic cells comprising ~90,000 m^2, e.g. a square area 300 m by 300 m, would be required (see Figs. 4 and 11).

A 25 m radius water-tower would thus be able to provide the 20 m^3 s^{-1} volumetric flow of water at night for 3272 s, e.g. ~55 min. Re-filling the water tower might be aided slightly by a mica-sheet funnel that could unfold as an inverted umbrella system at the top of the water tower to catch rainwater or condensation at night. The folded device might rest in the central pipe section of the spherical water-reservoir or be stored in the ground and raised when needed to capture the rainwater. It may also be possible to line the water tower with the heat-pipe units as mentioned earlier. The energy transferred by the heat-pipe generator-set could be from a parabolic mirror that transfers both solar photovoltaic and thermal energy. The two would have maximum efficiencies of 14 and 26% respectively [12,58].

9. Photovoltaic power from the Sun

The Sun delivers 1385 W m^{-2} to the Earth's upper atmosphere and approximately on average in Britain it reaches 1000 W m^{-2} during sunshine hours (see Fig. 12, [49]. The use of such energy might be for its direct conversion, its storage for subsequent generation of electricity, or its use for the conversion of carbon and hydrogen compounds into a hydrocarbon fuel for OCGT and CCGT use. Tables 6 and 7 compare PV and thermal energy possibilities.

It is well known that coatings of thickness equal to one quarter the wavelength of the light will reflect part, i.e. 38%, of the flux of a particular desired wavelength as long as the refractive index of the coating exceeds the refractive index of the glass substrate [60]. Multiple coatings can result in nearly a 100% reflection effectiveness.

A glass layer coated with a layer of monocrystalline PV cells can be inserted near the focal spot of the primary parabolic mirror. This will allow approximately half of the insolation of the PV-generating wavebands (see Fig. 12) to be concentrated. Alternatively, a monocrystalline (0.8 micron band) silicon-coated-glass PV cell unit can form a surrounding cylindrical enclosure to this layer (see Fig. 13). This second cylindrically-shaped unit rests upon the primary parabolic mirror rim while itself

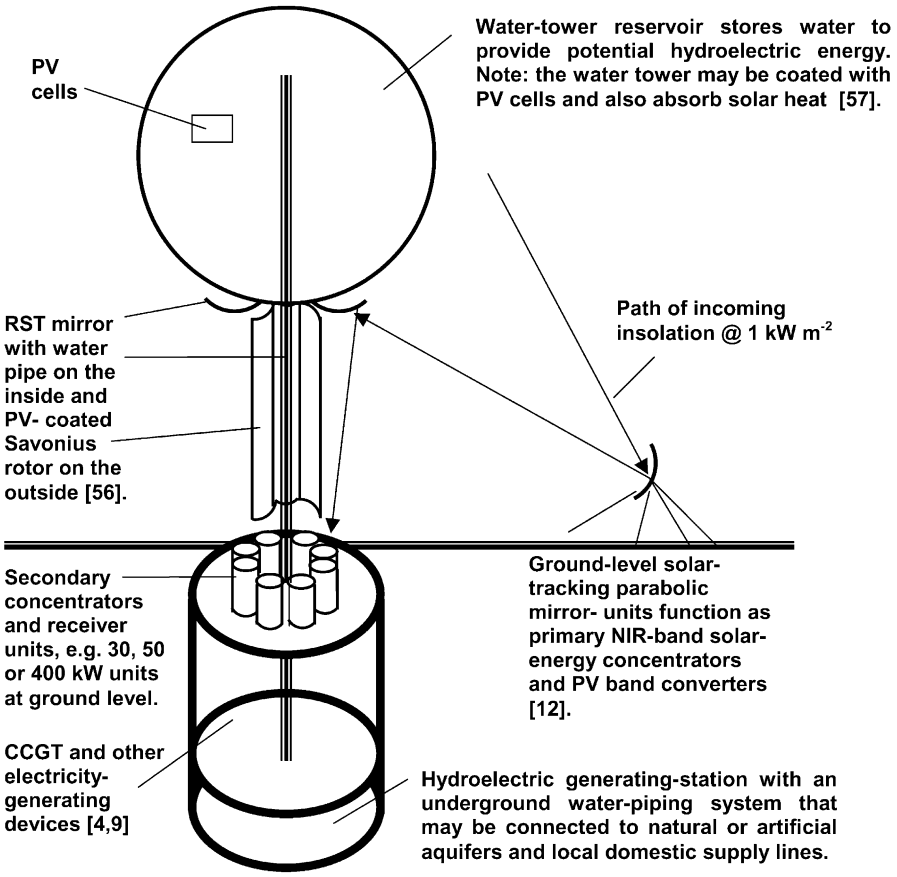

Fig. 11. One form of CPP plant. Here a $\lesssim$31% efficient Savonius rotor transfers wind energy to an electricity generator, while a $\sim$30% efficient parabolic mirror system transfers solar heat to a CCGT. Photovoltaic concentrators transfer PV energy with an efficiency that ranges from 14 to 30% for multi-coated cells. When supply exceeds demand, any excess electricity produced can be stored as potential energy in the form of water at an elevation, e.g. in the tower reservoir. Falling water can subsequently be harnessed to generate electricity as well as supply water [4,9,12,56,57].

supporting an amorphous (0.55 micron band) PV cell-layer cover to the unit (see Fig. 13).

The concentration that modern monocrystalline PV cells can tolerate is up to 500 times the normal insolation [64,67]. This concentration characteristic will allow up to a 99% saving in area, weight and cost of the solar panels. The efficiency of monocrystalline cells at 300 times the normal insolation is 26% [64]. It may be viable, at some future date, to harness the PV cells, electric resistance heating by using extra heat pipes— see component 12 in Fig. 7; and Fig. 9a and b [68].

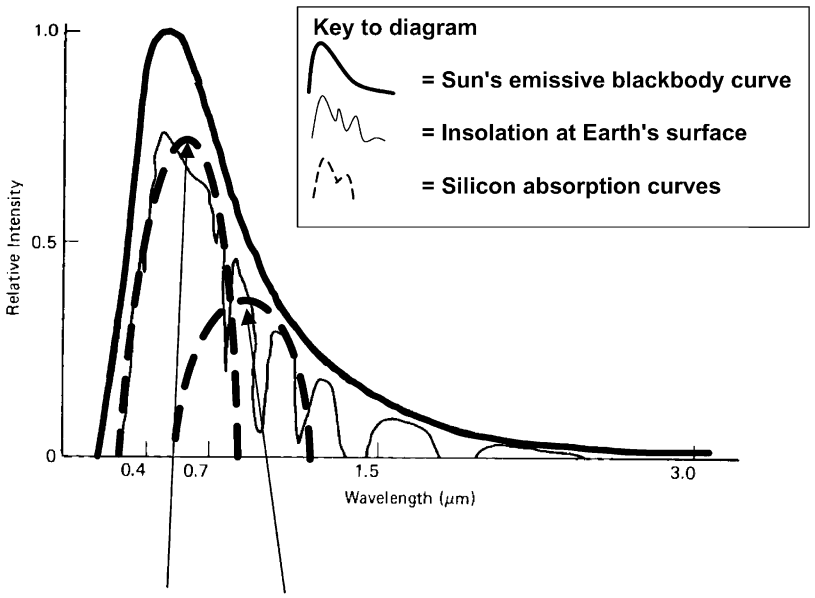

Fig. 12. Wavelength distribution of the insolation. The upper curve is the ideal black-body curve for the Sun's emissions. The lower curve indicates what is left after the attenuation in intensity of the solar spectrum due to the Earth's atmosphere. The dashed curves depict the intensity versus wavelength for the spectral responsivity of amorphous and mono-crystalline silicon PV cells respectively. Arrows point to peak wavelengths where the two PV cell-types of silicon absorb with ~90% efficiency, e.g. at ~550 and 800 nm [49].

10. Combined PV and NIR power-transfer

The concentration-ratio maximum for a working PV monocrystalline cell can be approximately 300:1 (see Fig. 14 for representative behaviour).

A maximum insolation of 1 kW m^{-2}, with a concentration potential of 300:1, might possibly be concentrated onto an area 33.2×10^{-4} m^{-2}, e.g. a 6.5 cm diameter surface. In practice, losses are incurred because the Fresnel lens used occupies a larger area than the PV cell it overlies and thus only <120 W m^{-2} of useful power is likely to be the forthcoming commercial output [64].

Table 6
Typical intake requirements and output characteristics for a commercially-available single-crystal photovoltaic cell system [49]

Wavelength responsivity 10^{-7} m	Average responsivity over solar spectral range $\frac{^{A}\text{Electricity}}{^{W}\text{Solar}}$	Open-circuit voltage (V)	Theoretical efficiency (%)	Average current density (Amp/m^2)	Power density (W/m^2)	Efficiency (output power/ Input power) (%)
4–11	0.4	~0.6	24	239	143	~14.3

Table 7
Characteristics of typical solar thermal-energy harnessing systems. Data should be compared with those in Table 6, e.g. from PV energy systems [9,59]

Energy-harnessing system:	Solar pond	Parabolic trough	Parabolic dish	Parabolic dish & CPC	RST/CCGT/ turbine	MHD/RST/ CCGT
Solar concentration	1	50	1000	10,000→30,000	10,000→30,000	10,000→30,000
Temperature °C	50→ <100	300→400	400→800	1200→1500	1200→1700	1700→2300
Net efficiency %	1	10	15	20	30	60

Hence, instead, it may be wiser to concentrate the flux with a parabolic mirror as in Fig. 13: a second (inverted) parabolic mirror may be used to reflect the primary's NIR energy rays (see component 5). This will enable high concentrations, i.e. usable working temperatures of 400–800 °C, to be achieved with a small mirror system [9]. There are two possible options that one may choose with regard to Fig. 13. Option 2 produces less overall power than Option 1 as the insolation is not concentrated, but would probably be cheaper and easier to manufacture than Option 1 at the moment. With Option 1, ~25% of the solar radiation may be absorbed by the amorphous cover-glass unit (see component 1 in Fig. 13) and ~25% of the remaining useful PV light may be concentrated by the primary mirror (component 3 in Fig. 13) onto the small monocrystalline unit (see component 6 in Fig. 13). Amorphous-silicon cell units may also be adapted to receive concentrated insolation. An amorphous coating may back the single-crystal coating (see component 6 in Fig. 13), but cost alone has prevented this innovation from reaching the market [69]. Sun-tracking (see component 10 in Fig. 13) attempts to keep the output at a maximum (but it incurs an extra capital cost).

Single-crystal silicon-cell efficiencies of up to 0.26 have been achieved [64]. Thus using Option 1 for the Fig. 13 system, the DIPPER unit could produce up to 3 kW, i.e. 260 W m^{-2} from five 10-cm diameter single-crystal silicon cells constituting component 6. With Option 2, the amorphous silicon cells might be placed on the cover (see component 1 in Fig. 13) and absorb ~25% of the insolation. A parabolic dish (see component 3 in Fig. 13) would then reflect ~75% of the remaining insolation towards a dichroic mirror (see component 4 in Fig. 13). The dichroic mirror could reflect another 25% of the insolation onto the single-crystal silicon cells on the side of component 2 in Fig. 13.

The remaining 50%, i.e. 500 Wm^{-2}, of solar thermal energy, might then be transferred to a heat-pipe generator-set (see components 7 and 8 in Fig. 13). Assuming a maximum efficiency of 0.8 for the heat-pipe generator-set (or the equivalent for a simple heat-pipe transferring the solar heat to another device), then ~60 W_e m^{-2} might be generated, as may be deduced using the shaft Eq. (2). A combined power output of approximately 400 W m^{-2}, i.e. a combined efficiency of 0.4 from both the photovoltaic units and the solar thermal-energy heat-pipe generator-set would be a goal for the designer to achieve. This will rise to >0.5 when multi-coated PV cells and parabolic mirror systems become relatively inexpensive.

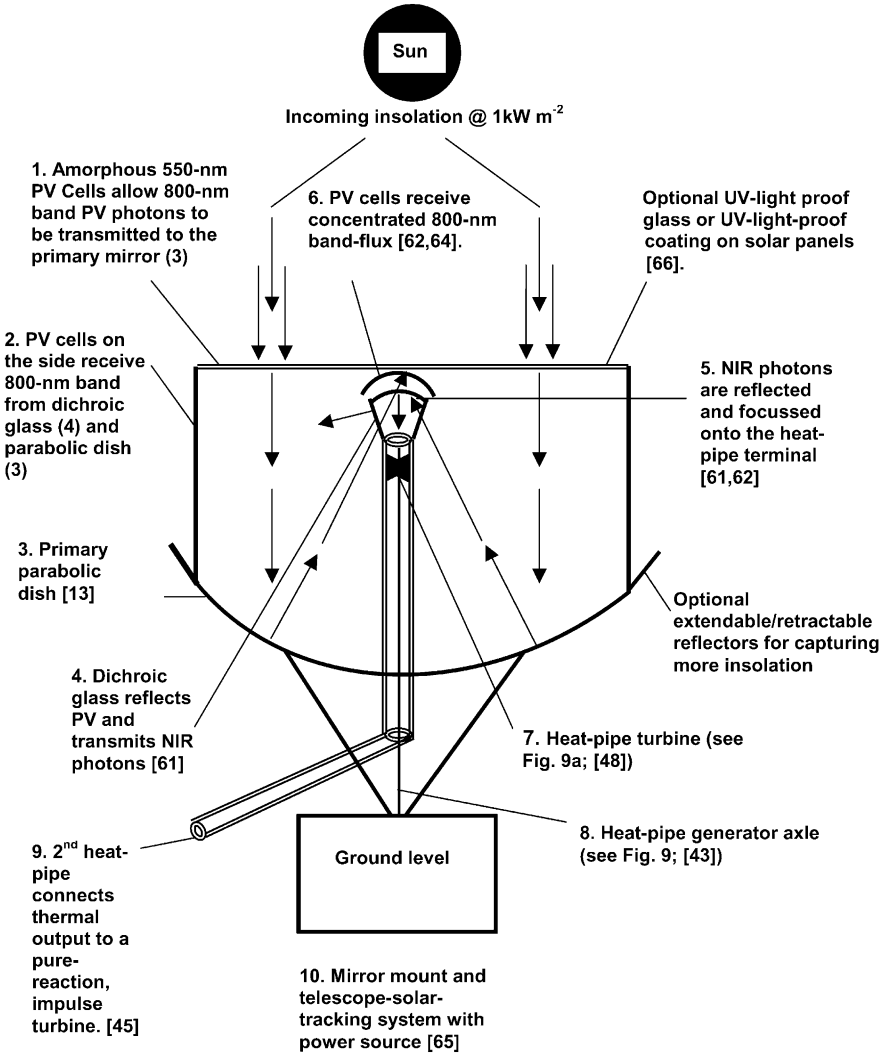

Fig. 13. A simple two-dimensional sketch of a possible double-irradiated photovoltaic and photon energy-relay (DIPPER) system. The PV photon-reflecting glass can be designed to reflect PV rays onto the PV cells [61] or concentrate them onto PV cells [62]. There are then 2 design options regarding separation and utilisation of both (550 and 800 nm band) PV and NIR band photons. An efficiency maximum of 0.6 is possible [12,63].

The total percentage of insolation that can be diverted to the PV cells to achieve a greater power output must be balanced against the total percentage of insolation that should be concentrated by the secondary dichroic mirror (see component 5 in Fig. 13) and transferred to the heat pipe (component 7). The performances of combined PV-thermal energy systems have been measured by Rekstad and Sandnes [70].

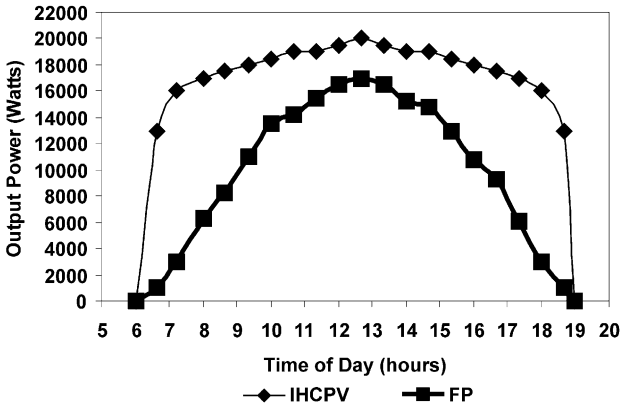

Fig. 14. Power output versus time of day for a 158 m^2 20 kW roof unit (top curve), e.g. a system of 300× concentration Fresnel lenses that produces 120 W m^{-2}. This low-overall output is due to cell-unit spacing requirements. IHCPV = power from integrated high-concentration photovoltaic (upper curve) and FP = power from flat-plate solar panel (lower curve). Note that, at noon, the maximum output of 20 kW is achieved, whereas a solar-tracking system such as in Fig. 13 would be nearer its maximum power rating for more of the sunshine hours [64].

They reported that the use of PV cells in combination with a thermal energy absorber only reduced by ~10% the absorber's maximum output. The heat pipe (see Fig. 9) could be used both to transfer heat to an engine (see component 9 in Fig. 13), such as a Stirling engine [13], or as a simple heat-transfer device [45].

It is possible to manufacture coatings of PV materials on either side of a glass substrate or directly on top of one another. A completed multi-layer solar-cell would have several layers of silicon types that would absorb insolation from different parts of the solar spectrum. It would be 100–200 microns thick, be coated with antireflection porous-silicon and have a reflective coating on the inside in order to lengthen the photon pathway. This increases the probability of photon (i.e. energy) absorption. Several layers of PV materials could bring the efficiency up to ~0.3 [63]. The 10.3 m diameter mirror mentioned earlier also has a maximum efficiency of ~0.3 [13]. This unit did not use the full potential of the insolation in that it made no use of the Sun's PV cell spectrum (see Fig. 12). The present analysis suggests that the efficiency of a prototype composite PV/thermal energy unit may approach 0.6. The development of composite units (e.g. with the Savonius rotor mentioned earlier) deserves further consideration.

11. An ideal large-scale CPP plant

Fig. 11 depicts what an optimal CPP plant might look like, i.e. one that can utilize solar, wind, water reservoir, and fossil fuel energy inputs. Each locality has available different intensities of economically-viable forms of renewable energy. However, it must be remembered that the only almost-perpetual source of energy is from

insolation and its potential to generate wind and hydroelectric power and, in the extremely long-term, even to re-generate fossil-fuel supplies.

12. Applications

The exhaust gases from the primary or secondary generator can have many applications. The most common, other than simple heating, is for secondary or tertiary generated electricity, which could in turn have many applications. One of present interest for the secondary-generated electricity is for stimulating a thruster fan at the nose of an aerofoil-shaped airship thereby facilitating its manoeuvring and docking prior to landing. Another recent application is the use of a maser cavity implanted in exhaust gas piping [71]. IR emissions from hot exhaust gases have been found to be theoretically capable of maser action, which in turn can create an inverted population of electrons in a laser cavity implanted in tandem with the maser in the exhaust-gas piping. It is alleged that the laser action will be of sufficient efficiency to make it worthwhile and so improve the overall efficiency of an Otto cycle.

The solar spectrum (see Fig. 12) can be split into distinct wavebands with the use of special filters and mirrors. This process permits the use of insolation to energise solid-state lasers [7]. The minimum insolation-concentration required is 300 times the normal insolation and the overall conversion efficiency from solar visual bands is 30%. Such solid-state lasers, e.g. those using Neodimium and Alexandrite, are tunable to the 800 and 550 nm absorption bands of single-crystal and amorphous silicon. An important outer-space application might be to energise distant solar-cell-powered satellites with high-density laser light.

13. Economic assessments of the considered systems

The primary-generation system cost, as evaluated in this report, is regarded as being composed of the capital cost of the solar concentrator, its mirrors, compressor, a CCGT, generator, along with the costs for any supplementary OCGT or CCGT fuel and maintenance for the first year of operation. This is a crude means to facilitate comparing approximate output costs for the primary, secondary, and tertiary generators. In practice, the economics of each proposed system will be more complicated and will depend upon (1) the unit value (p/kWh) of the electricity generated (which will vary with time) and (2) the lifetimes of the components.

Alone, any one of the considered cascade systems might not seem at first sight to be worthwhile. However, when combined in a large-scale version, e.g. as in Fig. 11, some of the multi-energy-input systems for electricity generation could, in the medium-term future, become viable practical possibilities [57]

In Table 8, the estimated first-year cost for running this large-scale hybrid generator-set is approximately 46 US cents/kWh. This discouraging result should be compared with an average (UK price) of 7.2 p/kWh at present peak-rates [73,74] for electricity from the "National Grid" for domestic power-consumption.

After the first year, the capital cost will disappear, if no borrowing was made initially, but the costs of parts, maintenance and probably the fuel will increase. Minor repairs will probably be necessary for the first 15 years, following the initial purchase, while major repairs may become essential during the second 15-year period of the 30-year predicted lifetime. The cost per kWh may decline in the first 5–15 years but will probably increase subsequently. The overall result should be that the average price over a 30-year period is likely to be close to the real current cost if methane reformation becomes cheap, or more likely it will increase when the predicted unit-fuel price hike for hydrocarbons occurs.

The total cost of the secondary-generation unit is composed of the costs of the secondary system's components. There are two possible types of turbine, which could be employed for the secondary system, i.e. the impulse or the reaction turbine. If the source temperature is approximately 600 °C and a large mass-flow exists, then use of the secondary system with a reaction turbine is viable. If the source temperature is approximately 1200 °C and a large mass-flow exists, then a CCGT (using low-grade energy) third-stage system, e.g. a pure-reaction, impulse turbine is the better choice. If the source temperature is 600 °C and a relatively small mass-flow exists, or below 600 °C with a large mass-flow, then the preferable system would be a pure-reaction, impulse turbine.

Secondary generation (Table 9) appears to be less expensive than primary generation (Table 8). This is because of the present estimated capital costs of the particular NIR/RST plant assessed, and would not be so for traditional primary generators. It is readily apparent that the advanced RST/CCGT unit, as depicted in Fig. 4 and Table 9, cannot be the primary generator, given the present economic situation.

Table 8
Deduced primary generation and annual costs at 1996 prices in US dollars for a hybrid solar-energy/CCGT system [72]

Gas turbine and solar plant capital costs	\$76,300,000
69 GWh per year from CCGT gas-energy at night 72 GWh per year from solar energy harnessed during the day 37 GWh per year from gas and solar energy used for periods near sunrise and sunset	
178 GWh total power	Hybrid system
Local Israeli Sunlight hours: 3208 per year Net solar power: 109 GWh/3208 h Electrical output	34 MW_e
Annual running costs: (1996 prices)	
Fuel	\$3,291,000 (gas)
Parts, wages and maintenance	\$2,258,000
Total: capital + first year of operation	\$81,849,000

The capital costs for secondary generation are assumed disappear after the first year in a similar manner as with the primary-generation system, but the maintenance costs may rise, e.g. the heat-exchangers may need cleaning (at a frequency depending upon the rate of soot deposition, if supplementary hydrocarbon fuels are used) and their lifetimes are estimated to be five years by the manufacturer [75]. The average cost per kWh per year should then decrease to approximately half the evaluated and then level out according to the earlier-mentioned maintenance-dependent costs. For larger mass flows, e.g. greater than 1 kg s^{-1}, the efficiency and thus the power generated per unit cost increases [17].

For the tertiary system, using the pure-reaction, impulse turbine, Table 10 lists the basic costs.

From Table 10, it can be seen that the typical electricity-generation cost for this tertiary generator is 78 p/kWh. The unit price may come down if such assemblies went into mass production and there may be some savings in cost and increases in electrical output if two (or more) units can be made to operate in parallel. The system's life is estimated to be approximately 5 years, e.g. due to the wear of the components such as the bearings. Because some of the components are being used intensively and there is only a 1-year guarantee on most commercial components, the system will also need continuous monitoring and frequent maintenance.

Thus the tertiary-generation cost is excessive at this juncture and so this system is unlikely to be adopted except in extreme cases, where the thermal signal has to be suppressed, e.g. for unmanned electrically-driven military spy aircraft or where fire hazardous conditions prevail.

Table 9
Secondary-generation systems' estimated costs as capital investment and first-year running costs, i.e. for a low mass-flow (<1 kg s^{-1}) system

1st system: Impulse turbine capital-costs	£25,000
Generator's (100 kVA mp) capital-costs	£1350
Heat-exchanger's capital-costs	£3000
Feed-pump system's capital-costs	£1000
Maintenance: parts plus part-time wage for first year	£2000
2nd System: reaction turbine capital-costs	£25,000
Generator's (100 kVA mp) capital-costs	£1350
Gas-to-liquid heat-exchanger's capital-costs	£8000
Gas-to-gas heat-exchanger's capital-costs	£10,000
Condenser's heat-exchanger capital-costs	£3000
Feed-pump system's capital-costs	£1000
Maintenance: parts plus part-time wage for first year	£2000
Total	
1st System	£32,350
2nd System	£50,350
Electricity generators' cost	
1st System	7.4 p/kWh @ 50 kW output
2nd System	11.5 p/kWh @ 50 kW output

Table 11 provides the costs for a single solar-energy-relay (DIPPER) system plus the running costs for the first year. These, as with the other costs within this report, should be used for comparative purposes only. Mass production might bring the costs down by as much as 70% if economies of scale prevail. The solar modules have 20–25 year guarantees concerning their capabilities of producing 80% of their maximum output power [58–78].

Table 12 depicts the estimated 25-year lifetime-costs for running the DIPPER system. Heat pipes last over 10 years in outer space, so the real cost concern is the relatively inexpensive £150 motor. This is because there are relatively-few moving parts in the DIPPER. The motor should last 5 years [65]. The cost of an additional heat engine to convert the NIR energy directly into electricity will be the major cost factor to consider (if the NIR energy is not required for space heating). The DIPPER, in effect, could become the primary generator for the RST/CCGT unit. This makes economic sense as the RST/CCGT unit "wastes" the potential PV energy that is available in the Sun's spectrum. As the cost of PV cells, in p/kWh, is presently decreasing while the unit costs of hydrocarbons are increasing (over the next 25 years), the DIPPER system would appear to be the only system that is economically viable at the present time.

Thus economies of scale for mass production of the DIPPER units plus new technology possibilities make this design interesting, e.g. it may be possible to layer the concentrated single-crystal silicon cell (Option 1 for Fig. 13) with an amorphous silicon cell. This could result in an increased total DIPPER photovoltaic conversion efficiency.

The pay-back period for the solar-CCGT system (Fig. 4) is estimated to be 30 years [9]. It is at present difficult to provide a worthwhile figure for the much longer pay back time of the tertiary generator (Fig. 7). However, the estimated lifetime of a DIPPER unit, i.e. which could energise the NIR/RST/CCGT unit, is only 5 years

Table 10
Tertiary generation estimated typical capital and annual costs

Cylindrical stainless-steel casing's capital-cost	£1000
Stainless steel boiler pipes' capital-cost	£3000
Turbine and generator axle's capital-cost	£1000
Generator's (100 kVA mp) capital-cost	£1350
Reaction-turbine's piping capital-cost	£1000
Turbine nozzles', diaphragms' and motors' capital-cost	£2000
Secondary impulse-turbine's capital-cost	£100
Secondary impulse-turbine's generator capital-cost	£1000
Feed pump's capital-cost	£350
Mirror concentrator's capital-cost	£500
Ethanol, conduction probes, acoustic transducer (for test prototype) capital-cost	£1100
Heat pipes' and fan's total capital-cost	£900
Maintenance: parts plus wages for first year	£500
Total:	£13,800
Electricity cost	
78 p/kWh @ 2 kW output	

Table 11
Estimated typical capital costs plus running costs for the first year for a Double-Irradiated Photovoltaic and Photon Energy-Relay (DIPPER) system running in southern UK (see Fig. 13)

Primary composite parabolic mirror's (~12 m^2 area) capital-cost		£2400
Aluminium layer with silicon monoxide coating (@ £200 m^2) capital-cost		£2400 [76]
Secondary parabolic-mirror's (Option 2) capital-cost (Aluminium layer with silicon-monoxide coating)		£50 [76]
Anti-UV light glass capital-cost (Options 1 or 2)		£500
Reflective mirror: capital-cost		
Option 1 @ 80 cm^2 (transmits PV wavelengths)		£781 [62]
Option 2 @ 100 cm^2 (transmits IR wavelengths)		£2000 [61]
Heat-pipe's capital-cost		£500
Turbine's and generator-axle's capital-cost		£500
Samarium-cobalt magnets. 20 (10 mm diameter × 2 mm), capital-costs		£232 [77]
Option 1 Marlec PV modules, ~1.2 kW (X 1)[a]		£7896 [69]
Option 1 Amonix PV cell, ~3 kW (X 300)[a]		£200
Option 2 Dulas cells, ~1.425 kW (X 1)[a]		£4351 [58]
Option 2 Heliostechnology cells, ~18 kW (X 1)[a]		£5070 [78]
Mount and tracking-motor's capital-cost		£700 [79]
Maintenance: parts plus wages for first year		£100
Total:	Option 1:	£16,209
	Option 2:	~£12,514
Insolation (in southern UK)		~8 kWh day^{-1}
Electricity cost for first Year: @ 8 h per day insolation		
Option 1: @ 6 kW maximum		~92 p/kWh
Option 2: @ 6 kW maximum		~70 p/kWh

[a] X 1 and X 300 refer to concentration ratios. Prices are at AD 2002 levels.

less, i.e. 25 years. A small-scale insolation-energised primary-generator unit (Fig. 13) is estimated to have a payback period exceeding 15 years (see Table 12), assuming with the present AD 7.2 p/kWh cost of electricity from the "National Grid" [74]. Mass production may reduce this pay back time, but such speculation is currently inopportune.

Table 12
A table of simple additional 5-year running costs used in order to estimate possible savings over a 25-year period for the Dipper system (without a heat-engine connected)

Dipper system Option 1	1st–5th year	6th–10th year	11th–15th year	16th–20th year	20–25th year	Total
Cost per 5-year period	£16,209 (1st year)	£500	£500	£500	£500	£20,209
Accumulated cost	£18,209	£18,709	£19,209	£19,709	£20,209	£20,209
Cost in p/kWh	92	2.9	2.9	2.9	2.9	
Accumulated cost in p/kWh	21	11	7.3	5.7	4.6	4.6

14. Conclusions

A three-stage cascaded electricity-generator may come into existence when world stocks of harnessable crude-oil become severely depleted [14,15]. However a two-stage CPP system may be an incremental innovation worth developing [80]. A single parabolic-mirror stage unit that converts solar energy directly to electricity via photovoltaic cells and via a heat-pipe generator-set might be cost-effective even now, e.g. for domestic purposes, in comparison with a solar concentrator CCGT-steam turbine unit.

The idea of a superfamily of design variants, e.g. single, double or triple stage systems, which can supply the demand for electricity for different levels of consumer need, is now a technical possibility. This has been made possible due to the recently achieved understanding of the optimisation of parabolic mirrors, heat pipes, the 85% efficient CCGTs, and multi-coated flux-concentrated PV cells.

The entire 2 (or 3)-stage assembly could be incorporated as a single plant. The new CCGT turbines' efficiency can be ~85% [81]. Secondary and tertiary generation could add a further 5 and 1% respectively to the overall conversion. Thus the total conversion could be approximately 90%. Alternatively, assuming that the predicted CCGT efficiency of 85% is achieved, then a 1st coupled directly to a 3rd stage unit could become a viable economic proposition, e.g. assuming that economies-of-scale apply to the pure-reaction, impulse turbine manufacturing costs. In this scenario, the (proposed) DIPPER (Fig. 13) would provide PV energy and transfer NIR energy to the RST/CCGT.

In reality, consumer needs for a large-scale electricity supply will dictate whether a large solar-energised CCGT system with an auxiliary methane reformer can be used, e.g. for demands where the electricity supply is much closer to 34 MW_e (Table 8) if the costs for an RST/CCGT system can be reduced. For small-scale consumer needs, e.g. (portable) 2–6 kW units, a small collection of PV cell and NIR-energy mirror-systems could be used.

The unit costs for electricity as deduced in this feasibility study are relatively high compared with those for large-scale commercial suppliers of electricity. This is partly because economies of scale for national supplies apply [82]. The extremely high generation costs of the tertiary stage (Fig. 7) together with its low contribution to

total gross power production makes it unlikely to be adopted. For the representative example considered (Fig. 4), primary generation may provide 34 MW_e (Table 8) of the total power production, but at an excessively high cost. Secondary-generation (Table 3), could contribute 500 kW kg^{-1} of steam (mass flow) utilised, but the unit may not be necessary if the new CCGTs (at ~85% efficiency) are utilised. The corresponding tertiary generation system and the photovoltaic and thermal energy relay (DIPPER) mirror systems would contribute only 2–6 kW respectively per system (Tables 10 and 11), and would probably have maximum efficiencies of 1 and 60% respectively. This relatively-high efficiency, i.e. of 60%, would enable the DIPPER system to be able to compete on the market with diesel and petrol-fuelled internal-combustion engines as suppliers of electricity where small amounts, e.g. 6 kW units, are required (and where a relatively-high daily insolation exists).

These values have been deduced assuming zero energy costs for the secondary and tertiary generation, because solar energy, methane (or carbon from CO_2) reformation and "waste" heat from the gas turbine satisfy these required inputs.

In general, the DIPPER's potential to work with a large-scale CCGT (Figs. 4 and 11), or on its own as a portable unit make it likely to be adopted in practical applications because of its relatively long lifetime (20–25 years) compared with its payback time of 15 years (see Table 12). Therefore, occasionally, under special circumstances, e.g. with the cheap mass-production of photovoltaic coatings and thermal-energy transfer mirror-systems (Fig. 13), auxiliary generation from solar energy could be worthwhile.

In order to improve the performance of the proposed system, cheap higher-temperature tolerant materials need to be developed because those used at present are near their metallurgical limits for this exercise. If we were to attempt to convert solar power to electricity on a large scale, e.g. to supply the total annual planetary electrical-demand of 100,000 teraWatt-hours, the objective must be to utilise silicon in the form of amorphous, porous, polycrystalline or monocrystalline units, because silicon is the only appropriate element available in the Earth's crust [44]. At the present time, it would appear that the cheapest form of electricity production from fossil fuels and insolation may be from large-scale CCGTs and small-scale insolation-harnessing systems that utilise both the PV and NIR energies of the Sun.

References

[1] Pope, C., No pilot necessary, Professional Engineer, pp. 45–46, July 24th 2002.
[2] Horlock JH. Combined power plants. Oxford: Pergamon Press, p xiii; 1992.
[3] Rameau F. Assessment of a CHP plant and thermal store supplying district heating to dwellings. Cranfield University, Cranfield, Great Britain, MSc thesis, 1995.
[4] Karni J, Doron P, Fiterman A, Kribus A, Rubin R, Sagie D. The DIAPR: a high-pressure, high-temperature solar receiver. Trans ASME, Solar Energy Engineering 1997;119:74–8.
[5] Horlock JH. Cogeneration: combined heat-and-power. Oxford: Pergamon Press; 1987.
[6] Sirchis J. Combined production of heat and power (Cogeneration). Oxford: Elsevier Applied Science; 1989.

[7] Kagan Y, Krupkin V, Yogev A. Non-imaging optics and solar lasers at the Weizmann Institute. Presented at the SPIE 38th International Symposium on Optical Applied Science and Engineering, San Diego, 11–16 July, 1993.
[8] Kribus A. High-concentration solar-energy optics. "Sun Day" Symposium, Weizmann Institute of Science, Rehovot, Israel, 1996.
[9] Kribus A. A high-efficiency triple cycle for solar-power generation. Solar Energy 2002;72(1):1–11.
[10] Ishigai S. Steam-power engineering. Cambridge: Cambridge University Press; 1999.
[11] British Meteorological Office. Sunshine statistics 1961–1990. Bracknell, UK: British Meteorological Office; 2002.
[12] Leonard JA. Solar thermal parabolic-dish systems technology and applications, SANDIA 84–9514. Albuquerque: Sandia National Laboratories; 1984.
[13] Washom B. Parabolic-dish stirling-module development and test results. SANDIA 84–9516, Advanco Corporation, Rancho Mirage, California, pp 1686–1693, 1984.
[14] Ion DC. Availability of world energy resources. London: Graham & Trotman Ltd; 1980.
[15] Goldemberg J, Johansson TB, Reddy AKN, Williams RH. Energy for a sustainable world. New York: Wiley Eastern Ltd; 1988.
[16] Webster R. Steam turbines. KKK Ltd., Northampton, UK, Personal Communication, 2001.
[17] Came P. Rodgers S. Impulse and reaction turbine data. PCA Engineers, Lincoln, UK, Personal Communication, 2001.
[18] Brown-Boveri Ltd. Steam turbines. Switzerland: Baden; 2001.
[19] Haywood RW. Thermodynamic Tables in SI (metric) Units, 3rd ed. Cambridge: Cambridge University Press; 1990.
[20] Silver RS. An approach to a general theory of surface condensers. Proc Instn Mech Engrs 1963/4; 178:339–57.
[21] Mori Y, Hijikata K, Hirasawa S. Optimized performance of condensers with outside condensing surface. Condensation Heat Transfer, Proc. of the 18th national Heat-Transfer Conference, San Diego California, pp. 55–62, August 6–8, 1979.
[22] Mayhew YR, Rogers GFC. Thermodynamic and transport properties of fluids, 5th ed. Oxford: Blackwell; 1998.
[23] Brown N. Generator datasheet. Cummins Ltd., Stamford, Lincolnshire, UK, Personal Communication, 2000.
[24] Lee MJ, Tien DL, Shao CT. Thermophysical capability of ozone-safe working-fluids for organic Rankine-cycle system. Heat- recovery Systems and CHP 1993;13(5):409–18.
[25] Meyer ML, Linne DL, Rouser DC. Forced-convection boiling and critical heat flux of ethanol in electrically-heated tube tests. In: 36th Aerospace Sciences Meeting and Exhibition sponsored by the American Institute of Aeronautics and Astronautics, Reno, Nevada, AIAA-98–1055, January 12–15, 1998.
[26] Kaye GWC, Laby TH. Tables of physical and chemical constants, 15th ed. London: Longmans; 1986.
[27] Perry RH, Green DW. Chemical engineer's handbook, 7th ed. New York: McGraw-Hill; 1997.
[28] Badr O, Probert SD, O'Callaghan PW. Selecting a working fluid for a Rankine-cycle engine. Applied Energy 1985;21:1–42.
[29] Aldrich Chemical Company. The Aldrich library of FT-IR spectra. Milwaukee, Wisconsin: Aldrich Chemical Company; 1997.
[30] Webb C. Lasers. Clarendon Laboratory, Oxford, UK, Personal Communication, 2000.
[31] Levy J. Prediction of two-phase critical flow rate. Journal of Heat Transfer 1965;87:53–8.
[32] Jones O. In: Lahey R, editor. Boiling heat transfer. Oxford: Elsevier; 1992. p. 1–30.
[33] Griffith PA. The prediction of a low-quality boiling void. ASME paper 63-HT-20, 1963.
[34] Spedding PL, Nguyen VT. Hold-up in two-phase gas-liquid flow: (A) theoretical results, (B) experimental results. Chem Eng Sci 1977;32:1003–10021.
[35] Badr O, Probert SD, O'Callaghan PW. Optimal design and operating conditions for a multi-vane expander. Applied Energy 1986;24:1–27.
[36] Walters PT. Wetness and efficiency measurements in LP turbines with an optical probe as an aid to improving performance. Trans ASME, Journal of Engineering for Gas Turbines and Power 1987; 109(1):85–91.

[37] Kearton WJ. Steam-turbine theory and practice. London: Pitman and Sons; 1945.
[38] Addison H. Applied hydraulics. London: Chapman and Hall Ltd; 1948.
[39] Hemingway TK. Electronic-designer's handbook. London: Business Books Ltd; 1970.
[40] Hill W, Horowitz P. The art of electronics, 2nd ed. Cambridge: Cambridge University Press; 1989.
[41] Hughes E. Electrical and electronic technology. 8th ed. Harlow: Prentice Hall, New Jersey; 2002.
[42] Harman PM. The scientific letters and papers of James Clerk Maxwell, Vol. 2, 1862–1873. Cambridge: Cambridge University Press; 1995.
[43] Dunstan D, Probert D. Increasing electricity generation per unit of fossil fuel so expended in diesel engines. Applied Energy 2001;70:267–80.
[44] Andersson BA, Azar C, Holmberg J, Karlsson S. Material constraints for thin-film solar cells. Energy, Vol. 23, No. 5, pp 407–411, 1998.
[45] Chisholm D. The heat pipe. London: Mills and Boon Ltd; 1971.
[46] Curtis EM. Heat pumps. R/M/N786, Central Electricity Generating Board, Marchwood Engineering Laboratories, Southampton, 1976.
[47] Belessiotis V, Mathioulakis E. A new heat-pipe type solar domestic hot-water system. Solar Energy 2002;72(1):13–20.
[48] Batty W. Heat transfer. School of Engineering, Cranfield University, Personal Communication, 2001.
[49] Wieder S. An introduction to solar energy for scientists. New York: John Wiley and Sons; 1982.
[50] Baker K, Chow LC, Gu CB, Pais MR. Vaporization heat-transfer of dielectric liquids on enhanced surfaces covered with wicks. AIAA-93–2835, pp 1–5, 1993.
[51] Shlosinger AP. Heat-pipe devices for space-suit temperature control, NASA/CR-1400. Washington DC: NASA; 1969.
[52] Open University. Introduction to thermofluid mechanics, Block 6. Milton Keynes: Open-University Press; 1996a.
[53] Simmons DM. Wind power. Park Ridge, New Jersey: Noyes Data Corporation; 1975.
[54] Cheremisinoff PN, Regino TC. Principles and applications of solar energy. Ann Arbor: Ann Arbor Science; 1978.
[55] Alexander G. Turbine efficiency. Faculty of Technology, The Open University, Milton Keynes, UK, Personal Communication, 1999.
[56] Park J. The wind-power book. Palo Alto: Cheshire Books; 1981.
[57] Larkworthy M. Combined-unit energy-systems. Thermal Engineering International, Wakefield, UK, Personal Communication, 2001.
[58] Knight J. Solar modules. Dulas Ltd., Machynlleth, Powys, Wales, UK Personal Communication, 2002.
[59] York T, Golding P, Sandoval J. Progress in solar ponds. Proceedings of the 3rd international conference, University of El Paso, El Paso, USA, May 23–27, 1993.
[60] Young HD. University physics. Reading, US: Addison-Wesley; 1992.
[61] Munday R. Dichroic mirrors. Advanced-Technology Coatings, Great Britain, Personal Communication, 2002.
[62] Maher K. Dielectric coatings. Linos-Photonics, Milton Keynes, UK, Personal Communication, 2002.
[63] Open University. Innovation and design, Block 2, readings and case studies. Milton Keynes: Open-University Press; 1996b.
[64] Garboushian V, Roubideaux D, Yoon S. Integrated high-concentration PV near-term alternative for low-cost large-scale solar power. Solar Energy Materials and Solar Cells 1997;47:315–23.
[65] Rees P. Telescope tracking. Telescope Technologies, Birkenhead, Liverpool, UK, Personal Communication, 2002.
[66] Horsly M. UV-light proof glass. Pilkington Special Glass, St. Asaph, Denbighshire, UK, Personal Communication, 2002.
[67] Bowden S, Dickinson M, Green MA, Honsberg CB, Largent R, Shaw N, et al. Low-cost photovoltaic roof tile. Solar Energy Materials and Solar Cells 1997;47(1–4):325–37.
[68] Akbarzadeh A, Wadowski T. Heat pipe-based cooling systems for photovoltaic cells under concentrated solar-radiation. Applied Thermal Engineering 1996;16(1):81–7.

[69] James S. PV modules. Marlec Ltd., Northamptonshire, Great Britain, Personal Communication, 2002.
[70] Rekstad J, Sandnes B. A photovoltaic/thermal (PV/T) collector with a polymer absorber plate, experimental study and analytical model. Solar Energy 2002;72(1):67–73.
[71] Scully MO. Quantum afterburner: improving the efficiency of an ideal heat-engine. Physical Review Letters 2002;88(5):50.
[72] Spharim I. The economics of the solar-reflective tower. "Sun Day" Symposium, Weizmann Institute of Science, Rehovot, Israel, May 1996.
[73] IEA. Electricity information. OECD/IEA, section ii pp 661–679, 2000.
[74] Baker S. Electricity rates. Office of Gas and Electricity Marketing, Great Britain, Personal Communication, June 2001.
[75] Bowman's Ltd. Heat-exchangers. Birmingham, Great Britain, Personal Communication, 2001.
[76] Pearce J. Mirror coatings. Vacuum Coatings Ltd., London, UK, Personal Communication, 2002.
[77] Goodfellows. Samarium cobalt magnets. Cambridge, Great Britain, 2002.
[78] Campagnolo L. Photovoltaic modules. Heliostechnology, Carmignano di Brenta, Italy, Personal Communication, 2002.
[79] Farnell Electronic Components Ltd. Motors. Leeds, Great Britain, 2002.
[80] Babus'Haq RF, Probert SD. Combined heat-and-power market-penetration in the UK: problems and opportunities. Applied Energy 1994;48:315–34.
[81] Ivey P. CCGTs. School of Engineering, Cranfield University, Personal Communication, 2001.
[82] Jackson T, Oliver M. The market for solar photovoltaics. Energy Policy 1999;27(7):371–85.